Research Square

Preprints are preliminary reports that have not undergone peer review.
They should not be considered conclusive, used to inform clinical practice,
or referenced by the media as validated information.

Bacterial community structure and plant growth-promoting traits associated with cluster roots of Gevuina avellana (Proteaceae) in soils with contrasting aluminum availability

Graciela Alejandra Berríos

gberr001@gmail.com

Universidad de La Frontera https://orcid.org/0009-0008-7856-1533

Mabel Delgado
Vicente Arellano
Carla Sandoval
Claudia Rabert
Marcia Astorga
Héctor Herrera
Jaznine Sandoval
Giovanni Larama
Marjorie Reyes

Research Article

Keywords: Gevuina avellana, acidic soils, aluminum, cluster roots, metabarcoding, Al tolerant bacteria, plant growth-promoting bacteria

Posted Date: May 5th, 2026

DOI: https://doi.org/10.21203/rs.3.rs-9372040/v1

License: This work is licensed under a Creative Commons Attribution 4.0 International License. Read Full License

Version of Record: A version of this preprint was published at Plant and Soil on August 14th, 2026. See the published version at https://doi.org/10.1007/s11104-026-08973-y.

Abstract

Aims.

This study aimed to characterize the rhizosphere bacterial community structure associated with the cluster roots (CR) of the Al-accumulating plant, *Gevuina avellana* Mol.(Proteaceae) growing in soils with contrasting aluminum (Al) availability.

Methods.

Bulk soil (BS) and rhizosphere soil from CR and non-cluster roots (non-CR) were sampled at two natural sites with contrasting soil chemical profiles, especially regarding Al saturation: Oncol Park (75%, +Al site) and Rucamanque Park (0.5%, -Al site). Bacterial diversity and community structure were assessed using 16S rRNA gene metabarcoding analyzed with QIIME2, LEfSe and FAPROTAX. Additionally, Al-tolerant strains were isolated and screened *in vitro* for plant growth-promoting (PGP) traits.

Results.

Bacterial community structure was primarily shaped by site conditions rather than roots type. Proteobacteria and Acidobacteriota were the dominant phyla. The high-Al site was characterized by adapted taxa including Ktedonobacteraceae and *Candidatus Xiphinematobacter*, and the − Al site showed greater abundance of Al-tolerant strains. Isolates from both sites exhibited multiple PGP functional traits, such as phosphate solubilization and phytohormone production.

Conclusions.

This study demonstrates that soil chemical properties - particularly Al saturation, pH, and nutrient availability- rather than root type, are the primary drivers of bacterial community composition in *G. avellana* CR. The CR rhizosphere acts as a niche that selects for Al-tolerant, plant-growth-promoting bacteria (e.g., *Serratia* spp. and *Rahnella victoriana*), offering potential bioinoculants for acidic, Al-stressed soils. Further research is needed to validate these isolates for agricultural applications.

Introduction

Aluminum (Al) toxicity is one of the most widespread problems in acidic soils, affecting approximately 40% of the arable land worldwide (Barone et al. 2008). When soil pH decreases, insoluble Al forms are converted to soluble Al^{3+} ions, which are toxic to most microorganisms and plants (Kochian et al. 2015; Lemire et al. 2010). Al^{3+} inhibits root elongation by disrupting root apical cell structure, thereby affecting water and nutrient uptake (Kochian et al. 2015; Osawa et al. 2013). In addition, soluble forms of Al^{3+} strongly bind other soil elements, such as phosphorus (P), thereby decreasing their availability for plant nutrition (Kochian et al. 2004).

Most plants growing in acidic soils with high soluble Al levels have developed resistance mechanisms to avoid or tolerate the toxic Al^{3+} effects (Cristancho et al. 2011; Kochian et al. 2015). Plants adapted to high Al availability rely mainly on two strategies: i) exclusion of Al^{3+} from sensitive sites and ii) internal detoxification through complexation and sequestration (Kochian et al. 2004). Those plants that develop internal mechanisms to tolerate Al in large amounts (more than 1,000 mg kg^{-1} in their foliar biomass) are referred to as Al hyperaccumulators (Chenery 1948; Jansen et al. 2002). One main mechanism used by plants to prevent Al toxicity is the production of carboxylates. These organic compounds act as chelating agents that bind Al^{3+}, decreasing its bioavailability and preventing its deleterious effects on plant growth and development (Bojórquez-Quintal et al. 2017; Kochian et al. 2015). Additionally, it is well known that the exudation of carboxylates into the rhizosphere promotes the development of beneficial soil microorganisms (Ma et al. 2022), including bacteria that can contribute to plant tolerance to soils with acidic pH and high Al saturation (Zhang et al. 2022). Consequently, there is increasing interest in identifying and studying the mechanisms of Al^{3+} resistance in plants inhabiting acidic soils.

Plant tolerance to Al^{3+} stress can vary depending on the microorganisms that inhabit the rhizosphere (Mora et al. 2017). It is well known that Al^{3+} stimulates root exudation in plants and that these compounds act as substrates, signals and/or antimicrobials, stimulating microbial growth and chemotaxis in the rhizosphere (Chaparro et al. 2013; Morgan et al. 2005). Increased levels of

carboxylates not only regulate soil Al^{3+} concentrations (Silva et al. 2004), but also shape the microbial community composition at the root soil interface by providing readily available carbon sources (Bürgmann et al. 2005). Indeed, high Al concentrations in the rhizosphere, as well as other heavy metals, can directly affect microbial populations by altering their size, diversity and activity (Yu et al. 2014). Previous studies examining the rhizosphere bacterial community structure in Al-tolerant and Al-sensitive genotypes have shown that tolerant plants selectively recruit bacterial taxa capable of mitigating Al^{3+} phytotoxicity (Lian et al. 2019; Wang et al. 2013; Yang et al. 2012). Mechanisms of resistance to toxic metals in bacteria include the production of chelating agents, metal efflux systems, active or passive bioaccumulation, biotransformation of toxic metals into less toxic forms, adsorption to the cell wall, and the expression of metal stress-related genes (Ahemad 2019; Kavamura and Esposito 2010; Mora et al. 2017; Sukweenadhi et al. 2015). Among these mechanisms, siderophore production has been proposed as an effective strategy for metal detoxification. Indeed, bacteria isolated from volcanic soils, such as *Klebsiella*, *Serratia*, and *Enterobacter*, have the ability to form Al^{3+}-siderophore complexes to cope with Al stress (Mora et al. 2017).

In addition to metal tolerant bacteria, the rhizosphere harbors a wide range of bacteria that perform essential functions in plant nutrition, growth, and disease suppression (Durán et al. 2014; Ma 2017; Oleńska et al. 2020). These bacteria are collectively referred to as plant growth promoting bacteria (PGPB). PGPB belong to a heterogeneous group of beneficial bacteria inhabiting the rhizosphere, including both free-living and endophytic forms (Bashan et al. 2004). PGPB can exert their effects from early plant developmental stages through direct and indirect mechanisms (Sanhueza et al. 2024). Direct mechanisms include solubilization of essential nutrients and phytohormone production, whereas indirect mechanisms are mostly related to the biocontrol of phytopathogens (Sarker et al. 2022). In addition, PGPB can alleviate abiotic stress by modulating 1-amino-cyclopropane carboxylic acid (ACC) deaminase activity and regulating gene expression (Barra et al. 2019; Martínez et al. 2011).

In the native forests of southern South America, several tree species have developed mechanisms that allow them to grow and adapt to the limiting conditions of acidic soils, including high Al^{3+} availability. Species belonging to the Proteaceae family are able to grow across a wide range of soils, from nutrient-rich to nutrient-poor volcanic substrates, and under both high and low Al saturation conditions (Delgado et al. 2018). One of these species is the Chilean hazelnut (*Gevuina avellana* Mol.), an endemic tree of sub-Antarctic forests with a wide distribution in Chile (Medel and Medel 2000). It occurs between 35° and 45°S and from sea level to 700 m altitude (Medel et al. 2004). *Gevuina avellana*, like most members of Proteaceae, produces cluster roots (CR), a specialized root structure that actively exudes organic compounds, modifying the rhizosphere and enhancing the release of ionic forms of nutrients (Delgado et al. 2021; Lambers et al. 2006; Zúñiga-Feest et al. 2021). Previous studies have shown that the rhizosphere bacterial community structure associated with CR differ from those associated with non-CR (e.g. in *Lupinus albus* L.; Marschner et al. (2004) and from bulk soils e.g. three species of Banksia, Proteaceae; Marschner et al. (2005)). These distinct microbial associations are thought to contribute to the ability of these species to establish and persist in nutrient-poor soils, similar to *G. avellana* (Delgado et al. 2018). In addition, *G. avellana* has the capacity to accumulate Al in its leaves (> 3000 mg Al kg^{-1}) without showing symptoms of Al toxicity (Delgado et al. 2025; Delgado et al. 2019). Therefore, this species represents an excellent model to investigate the mechanisms that enable plant persistence in soils with high Al availability and low fertility. To date, most studies on *G. avellana* have focused on leaf traits associated with Al tolerance (Delgado et al. 2025; Delgado et al. 2019), and on the functioning of its CR (Delgado et al. 2021; Zúñiga-Feest et al. 2021). However, interactions between this species and soil microorganisms at the level CR remain largely unexplored.

In this context, we hypothesize that bacterial communities associated with CR differ from those of non-CR and BS, and that CR selectively recruit Al-tolerant bacteria with PGP traits. Therefore, in this study we characterize the bacterial community structure associated with CR in the Al hyperaccumulator *G. avellana* growing in native forests of southern Chile. In addition, the functional properties of bacterial isolates were tested *in vitro* to assess their potential plant growth-promoting traits. To our knowledge, this is the first study to identify the community structure of bacteria associated with the CR of *G. avellana* an Al-hyperaccumulator plant and to screen these bacteria for beneficial plant growth-promoting traits.

Materials and Methods

Soil collection and chemical analyses

Adult *G. avellana* plants growing in natural forests were sampled across different localities in south-central Chile, including Vilcún (38°40'51.3"S 71°51'18.5"W), Melipeuco (38°50'25.0"S 71°39'48.7"W), Oncol Park (39°42'01.1"S 73°19'34.0"W) and Rucamanque Ecological and Cultural Park (38°39'30.6"S 72°36'14.9"W). At each site, three composite soil samples were collected for chemical

characterization. Each composite sample consisted of a pool of three subsamples taken from the bulk soil within 1.5 m of individual *G. avellana* plants. The samples were analyzed for pH, available Al and macronutrients (Phosphorus (P), Nitrogen (N), Magnesium (Mg), Calcium (Ca), Sodium (Na), and Potassium (K)), following the protocols described by Sadzawka et al. (2004). This preliminary sampling aimed to identify representative sites with contrasting Al saturation levels, classified as high ("+Al") or low ("–Al"), for subsequent analyses.

Soil sampling of cluster roots (CR) and non-cluster roots (non-CR) rhizosphere, and bulk from selected sites

According to chemical analysis results of the study sites, the sites Oncol Park and Rucamanque Ecological and Cultural Park (from here on called Rucamanque) were selected because they exhibited contrasting Al saturation levels, where Oncol site correspond to "+Al site", with 75% of Al saturation, and Rucamanque correspond to "–Al site", with 0.5% of Al saturation. At Rucamanque, *G. avellana* is associated with mixed forest species such as *Nothofagus obliqua*, *Laurelia sempervirens*, *Persea lingue*, *Aextoxicon punctatum*, and *Eucryphia cordifolia*. In contrast, at Oncol site *G. avellana* is associated with evergreen species including *Saxegothaeae conspicua*, *Drimys winteri*, *Podocarpus nubigenus*, *Amomyrtus luma* and *A. meli*. The climate and the origin of soils are well described by López et al. (2025).

For each selected site, three rhizosphere samples were collected, each consisting of a pool of three subsamples taken from individual *G. avellana* trees, each one separated by at least 10 m apart. Rhizosphere soil was collected separately from mature cluster roots (CR) and non-cluster roots (non-CR). Mature CR were distinguished from other developmental stages (juvenile or senescent) based on their white coloration, rounded morphology, and the presence of nail-shaped rootlet tips (see photographic record in Delgado et al. (2024), Supplementary Material). To collect the rhizospheric fraction, soil was excavated to a depth of 20 cm around the trunk of *G. avellana* trees. Once mature CR and non-CR roots were identified, they were vigorously shaken to remove loosely adhering soil. The resulting rhizospheric soil was collected in sterile containers, kept on ice during transport, and stored at 4°C until further analysis. Similarly, samples of bulk soil (BS) were collected for comparisons. Additionally, segments of non-CR and mature CR were excised and stored in sterile saline solution within Falcon tubes for subsequent isolation and characterization of Al-tolerant bacteria.

Bacterial community analysis by 16S rRNA gene metabarcoding

The composition and structure of the bacterial community in rhizosphere samples (CR and non-CR) and BS were analyzed using a metabarcoding sequencing approach. Genomic DNA was extracted using the DNeasy PowerSoil® Pro Kit (Qiagen) following the manufacturer's protocol and stored at -20°C until further analysis. DNA integrity was verified by electrophoresis on a 1% agarose gel stained with GelRed, visualized under UV light, and its concentration was quantified using an Epoch 2 microplate reader (BioTek Instruments, Inc.). The V3-V4 region of the 16S rRNA gene was amplified with primers B341F and B806R and sequenced on an Illumina MiSeq platform in paired-end mode for 300 cycles.

The quality of raw sequencing reads was assessed and processed using the QIIME2 pipeline (Bolyen et al. 2019) with its integrated tools, as detailed below. Denoising was conducted using the DADA2 algorithm (Callahan et al. 2016) to eliminate sequencing errors and generate high-quality amplicon sequence variants (ASVs). To enhance quality filtering, read merging, and chimera removal, the first 18 bases of each read were trimmed, and forward and reverse reads were truncated at 290 and 200 bases, respectively. ASVs were then derived from the processed reads. Taxonomic classification was performed using a Naïve Bayes classifier trained on the SILVA 138 database (Quast et al. 2012), with the model constructed from sequences specific to the V3-V4 region targeted by primers B341F and B806R. Mitochondrial and chloroplast sequences were excluded from downstream analyses. To infer phylogenetic relationships among ASVs, a phylogenetic tree was constructed using the FastTree algorithm (Price et al. 2010) based on a masked sequence alignment generated with MAFFT (Katoh and Standley 2013).

To ensure comparable sequencing depth, microbial samples were rarefied to 13,078 sequences per sample. Alpha diversity, which quantifies within-sample microbial richness and evenness, was evaluated using multiple metrics calculated via the QIIME2 core-metrics-phylogenetic function: Shannon's diversity index (measuring species diversity and evenness), Faith's Phylogenetic Diversity (assessing phylogenetic richness), Observed Features (counting unique ASVs), and Pielou's Evenness (evaluating species distribution uniformity). These metrics were compared across sampling sites using the Kruskal-Wallis test, with significant differences further explored through Dunn's post-hoc test for pairwise comparisons. To investigate between-sample (beta) diversity, a Principal Component Analysis (PCA) and hierarchical clustering were performed based on the Aitchison distance matrix, which accounts for the compositional nature of microbial data by applying a centered log-ratio transformation. Community composition differences were statistically tested using permutational multivariate analysis of variance (PERMANOVA) (Anderson 2001) with 999 permutations on

the Aitchison distance matrix. All statistical analyses and visualizations were conducted using the vegan package (Oksanen et al. 2019) in R. Taxa driving group differences were identified using Linear Discriminant Analysis Effect Size (LEfSe) (Segata et al. 2011), employing the Kruskal-Wallis test followed by Wilcoxon rank-sum tests for pairwise comparisons, with a significance threshold of $P < 0.05$ and a linear discriminant analysis score cutoff of 2.0. Taxonomy-based functional profiles were predicted from 16S rRNA data using FAPROTAX (Louca et al. 2016) to infer microbial ecological roles. Differential abundance analysis was performed using the zero-inflated Gaussian mixture model (ZIGMM) implemented in the metagenomeSeq package (Paulson et al. 2013). This model explicitly accounts for sparsity by modeling excess zeros separately from non-zero log-transformed abundances, while adjusting for library size via cumulative sum scaling (CSS) normalization. Statistical inference is based on maximum likelihood estimation within the ZIGMM framework, improving sensitivity in sparse microbiome datasets.

Isolation and characterization of Al-tolerant bacteria

Samples of the rhizosphere of mature CR, non-CR, and BS of *G. avellana* collected at the two sites with contrasting percentages of Al saturation were used to isolate Al-tolerant bacteria on a specific culture medium.

To isolate rhizosphere bacteria, soil aggregates were removed from the mature CR by shaking each CR for 5 min in 50 mL sterile saline solution (0.85% w/v NaCl). Similarly, to isolate rhizosphere bacteria from the non-CR and BS samples, 5 g of soil was weighed and then 50 mL of sterile saline solution was added and shaken for 5 min. Culturable Al-tolerant bacteria were selected by plating serial dilutions of the extraction solutions on Luria-Bertani (LB) agar containing different concentrations of Al (0, 100, 200, 300 and 400 mg L^{-1}) and incubated at 27° C for 3 days according to the methodology described by Jiang et al. (2022) with some modifications. The pH of the culture medium was adjusted to 4.8, and $Al(NO_3)_3$ was added as an Al source. The $Al(NO_3)_3$ was filter sterilized (0.22 microns) and then added to the sterile medium. Bacterial growth on LB agar without Al at pH 7.0 and pH 4.8 was used as controls. Al-tolerant bacteria were those that grew on agar plates with Al concentrations greater than 100 mg L^{-1} (Mora et al. 2017). Strains were selected based on colony morphology (shape, color, and size) and Gram staining.

ERIC-PCR-based discrimination of bacterial isolates

The isolates were characterized using Enterobacterial Repetitive Intergenic Consensus Sequences (ERIC-PCR). The ERIC-PCR was performed as described previously by (Rafiee et al. (2000)), using 1 μL from extracted DNA, 1.5 mM of MgCl2, 10 pmol of primers ERIC1 (ATGTAAGCTCCTGGGGATTCAC), and ERIC2 (AAGTAAGTGACTGGGGTGAGCG), 1.0 U of Taq DNA polymerase (LGC Biotecnologia, Sao Paulo, Brazil), 5 X PCR buffer, and water to complete the total volume of 25 μL.

The PCR reactions were carried out with the following cycling conditions: denaturation 5 min at 95°C, 35 cycles, consisting of denaturation for 1 min at 94°C, annealing for 1 min at 52°C, and extension for 8 min at 65°C, followed by a final extension for 16 min at 68°C. The amplification products were detected by electrophoresis at 75 V for 1 h 15 min in 2% Agarose 1000 (Invitrogen Corporation, Carlsbad, CA, USA) gel stained with gel red (LGC Biotecnologia, São Paulo, Brazil).

Bacteria identification through 16S rRNA gene analysis

Partial sequencing of the 16S rRNA gene was performed for molecular identification of selected bacterial isolates. For this, genomic DNA from the bacterial strains was extracted and purified using a commercial DNA isolation kit Omega Bio-Tek (E.Z.N.A) according to the manufacturer's instructions. Then, the 16S rRNA gene fragments were amplified by PCR with the universal bacterial primer sets 27F (5´-AGA GTT TGA TCC TGG CTC AG-3´) and 1492R (5´-TAC GGY TAC CTT GTT ACG ACT T-3´), according to the methodology described by Peace et al. (1994). Subsequently, these samples were sequenced on an ABI 3730XL (Applied Biosystems) sequencer by Macrogen (Chile). The sequences were analyzed and identified using the NCBI-BLAST database (http://blast.ncbi.nlm.nih.gov/Blast.cgi).

In vitro screening of plant growth-promoting traits in bacterial isolates

Phosphate solubilization

The modified National Botanical Research Institute Phosphate (NBRIP) culture medium was used to assess phosphate solubilization from four sources: rock phosphate, tricalcium phosphate ($Ca_3(PO_4)_2$), iron phosphate ($FePO_4$), and aluminum phosphate ($AlPO_4$). The medium consisted of glucose (10 g L^{-1}), $MgCl_2$ (2.5 g L^{-1}), $MgSO_4$ (0.25 g L^{-1}), KCl (0.2 g L^{-1}), $(NH_4)_2SO_4$ (0.1g L^{-1}), agar (15g L^{-1})

with the insoluble phosphate source replacing the standard phosphate salt (5g L^{-1}) besides bromophenol blue was added to the culture medium (0.1g L^{-1}) as a pH indicator to enhance visualization of solubilization halos (Nautiyal 1999). After 48 hours of incubation, halo formation around the colonies was assessed. Initially, phosphate solubilization was evaluated qualitatively, by considering the presence or absence of halos as a positive result. Subsequently, a semi-quantitative analysis was performed by measuring the diameter of each halo and the corresponding bacterial colony and calculating the solubilization index (halo diameter / colony diameter).

Siderophore production

Siderophore production was assessed using agar plates supplemented with chrome azurol S (CAS) reagent, following the method described by Hu and Xu (2011). To prepare the CAS agar, 100 mL of CAS reagent was mixed with 900 mL of sterilized LB agar. Each plate was inoculated with four bacterial strains and incubated in triplicate. An uninoculated plate served as the negative control. After incubation at 28°C for three days, siderophore production was indicated by the appearance of an orange halo surrounding the bacterial colonies, as described by (Louden et al. 2011).

ACC deaminase

ACC deaminase activity was assessed using the method described by Dworkin and Foster (1958), with modifications (Penrose and Glick (2003). A liquid bacterial culture was first incubated for 24–48 hours in DF minimal medium containing: KH_2PO_4 (4 g L^{-1}), Na_2HPO_4 (6 g L^{-1}), $MgSO_4 \cdot 7H_2O$ (0.2 g L^{-1}), glucose (2 g L^{-1}), gluconic acid (2 g L^{-1}), citric acid (2 g L^{-1}), and $(NH_4)_2SO_4$ (2 g L^{-1}) as the nitrogen source. The medium also included the following trace elements: $FeSO_4 \cdot 7H_2O$ (1 mg L^{-1}), H_3BO_3 (10 µg L^{-1}), $MnSO_4 \cdot H_2O$ (11.19 µg L^{-1}), $ZnSO_4 \cdot 7H_2O$ (124.6 µg L^{-1}), $CuSO_4 \cdot 5H_2O$ (78.22 µg L^{-1}) and MoO_3 (10 µg L^{-1}). A portion of the grown culture was then transferred to fresh DF minimal medium containing 1-aminocyclopropane-1-carboxylic acid (ACC) as the sole nitrogen source and incubated for 5 to 7 days. Cells were harvested by centrifugation at 8,000 × g for 10 minutes at 4°C, washed several times with 0.1 M Tris-HCl buffer (pH 7.6), and the resulting bacterial pellet was resuspended in 0.1 M Tris-HCl buffer (pH 8.5). Cell lysis was induced by adding toluene, followed by the addition of ACC and incubation at 30°C for 15 minutes. The reaction was stopped by adding 0.56 M HCl. To quantify the amount of α-ketobutyrate produced, samples were centrifuged at 16,000 × g at room temperature. One milliliter of the supernatant was mixed with 800 µL of 0.56 M HCl and 300 µL of 2.4-dinitrophenylhydrazine (0.2% in 2 M HCl), and incubated for 30 minutes at 30°C. Then, 2 mL of 2 N NaOH was added, and absorbance was measured at 540 nm using a spectrophotometer. Quantification was expressed as micromoles of α-ketobutyrate per milligram of protein per hour (µmol α-ketobutyrate mg^{-1} protein h^{-1}). A standard curve was generated using known concentrations of α-ketobutyrate.

Indole Acetic Acid (IAA) production

IAA production by the selected bacterial isolates was determined following the methodology adapted from Meliani et al. (2017). Bacterial strains were pre-cultured in 3 ml of LB medium for 24 h at 30°C under orbital agitation (120 rpm). Subsequently, 0.5 mL of each culture was inoculated into 10 mL of DF minimal medium supplemented with trace elements, ammonium sulfate ($(NH_4)_2SO_4$), and 0.2 g L^{-1} of tryptophan. Cultures were incubated at 30°C for 48 h in the dark with continuous shaking at 120 rpm. After incubation, the optical density was measured at 600 nm, and the cultures were sequentially centrifuged at 7,500 rpm for 10 min, followed by a second centrifugation at 13,000 rpm for 10 min at room temperature. The resulting supernatants were acidified to pH 2.5-3.0 with 1 N HCl and extracted with ethyl acetate in a 1:2 (v/v) ratio. The extraction was repeated 2–3 times to ensure efficient recovery of the IAA. The pooled organic phases were evaporated under reduced pressure at 50°C using a rotary evaporator. The dried extracts were resuspended in 5 mL of ethyl acetate and filtered through 0.22 µm membrane filters prior to analysis. Quantification of IAA was performed by high-performance liquid chromatography (HPLC) using a reverse-phase C18 column (46 × 250 mm). The mobile phase was composed of methanol (40%) and an aqueous 1% (v/v) acetic acid solution (60%), delivered under isocratic conditions at a flow rate of 1.0 mL min^{-1}. A volume of 20 µL of each sample was injected, and detection was carried out at 280 nm. IAA concentration was determined using a standard calibration curve prepared with analytical-grade IAA (≥ 95% purity) dissolved in methanol at different concentrations.

Statistical analyses

Rhizosphere bacterial abundance (CFU mL^{-1}) was subjected to one-way ANOVA followed by Tukey's multiple range test for mean comparisons. All statistical procedures were executed in Sigma Plot v.12. Results were deemed significant when $P \leq 0.05$.

Results

Soil chemical analyses

The chemical characterization of soils associated with *G. avellana* revealed clear contrasts among the four sampling sites (Table 1). Oncol exhibited the most restrictive conditions, characterized by high Al saturation (75.3%) and elevated exchangeable Al (3.89 $cmol_c$ kg^{-1}), together with the lowest pH (4.7) and reduced CEC. In contrast, Rucamanque showed the lowest Al saturation (0.53%) and minimal exchangeable Al, along with the highest CEC and base saturation. Melipeuco also displayed very low Al saturation (0.54%) and a moderately acidic pH. Soils from Vilcun presented intermediate conditions, with moderate Al saturation (8.74%), low pH, and reduced CEC. Based on these results, the sites Oncol and Rucamanque were selected for further analysis. Hereafter, samples from Oncol and Rucamanque will be referred to as "+Al" and "–Al" sites, respectively.

Table 1
Chemical properties of soils collected from the natural habitats of Gevuina avellana. Each value represents the mean of three samples ± standard error.

Soil Properties	**Location**			
	Vilcun **38°40'51.3"S 71°51'18.5"W**	***Melipeuco*** **38°50'25.0"S 71°39'48.7"W**	***Oncol*** **39°42'01.1"S 73°19'34.0"W**	***Rucamanque*** **38°39'30.6"S 72°36'14.9"W**
N[a]	20.67 ± 2.96	12.66 ± 0.33	8.66 ± 0.67	19.0 ± 1
P[a]	6.0 ± 0.67	4.0 ± 0.0	4.0 ± 0.0	5.0 ± 0.33
K[a]	81.0 ± 18.1	94.0 ± 2.26	141.0 ± 10.34	156.0 ± 12.57
pH[b]	5.40 ± 0.04	6.01 ± 0.02	4.69 ± 0.08	5.89 ± 0.1
Organic Matter [c]	7.0 ± 1.0	10.33 ± 0.33	15.33 ± 2.19	12.3 ± 0.88
CEC[d]	7.46 ± 0.93	9.2 ± 0.9	5.08 ± 0.53	16.44 ± 2.3
K[d]	0.21 ± 0.05	0.24 ± 0.0	0.36 ± 0.03	0.4 ± 0.03
Na[d]	0.1 ± 0.01	0.11 ± 0.03	0.13 ± 0.02	0.18 ± 0.02
Ca[d]	5.41 ± 0.74	7.35 ± 0.06	0.31 ± 0.11	11.48 ± 2.0
Mg[d]	1.12 ± 0.75	1.45 ± 0.02	0.39 ± 0.07	4.3 ± 0.16
Al[d]	0.62 ± 0.18	0.05 ± 0.00	3.89 ± 0.7	0.07 ± 0.05
Al Saturation [c]	8.74 ± 2.57	0.54 ± 0.06	75.33 ± 6.29	0.53 ± 0.42
Base saturation	6.84 ± 0.99	9.15 ± 0.09	1.19 ± 0.18	16.37 ± 2.17

[a] $mg\ kg^{-1}$

[b] in H_2O

[c] %

[d] $cmol_c\ kg^{-1}$

Bacterial analysis by 16S rRNA gene metabarcoding

Soil samples from BS and the rhizosphere (CR and non-CR) of *G. avellana* growing under contrasting Al saturation were analyzed using 16S rRNA gene metabarcoding. The average relative abundance of bacterial taxa at the phylum and family levels was determined for all soil and rhizosphere samples collected from the + Al and –Al sites (Fig. 1A). Across both sites, the dominant bacterial phyla were *Proteobacteria* (ranging from 21.3 ± 2.8% to 28.3 ± 3.0% in + Al site, and from 24.4 ± 1.5% to 29.7 ± 6.0% in –Al site), *Acidobacteriota* (from 21.4 ± 3.9% to 26.7 ± 2.0% in + Al site, and from 19.0 ± 1.8% to 21.7 ± 2.6% in –Al site), and *Planctomycetota* (from 21.8 ± 2.6% to 24.6 ± 0.8% in + Al site, and from 17.8 ± 6.0% to 20.9 ± 0.9% in –Al site). These three phyla comprised most of the bacterial community composition across all samples. Phyla with moderate representation, reported as average values across sample types, included *Verrucomicrobiota* (10.6 ± 0.6% in + Al site and 17.6 ± 2.5% in –Al site), *Chloroflexi* (5.5 ± 2.9% in + Al site and 2.7 ± 1.4% in –Al site), and *Bacteroidetes* (3.2 ± 0.9% in + Al site and 4.7 ± 0.46% in –Al site). The remaining proportion corresponded to other phyla present at lower relative abundances. In rhizosphere soils of CR samples from the + Al site, *Chloroflexi*, WPS-2, and *Cyanobacteria* were found in greater proportions than in CR samples from the –Al site (Fig. 1A and Supplementary Table S1). At the family level, a higher relative abundance of bacterial taxa belonging to the Ktedonobacteraceae and Koribacteraceae was observed at the + Al site compared with the –Al site (Fig. 1B). In contrast, members of the Chthoniobacteraceae were more abundant at the –Al site than at the + Al site (Fig. 1B). Additionally, in the rhizosphere soils of CR samples from the + Al site, bacterial families such as Ktedonobacteraceae, Xiphinematobacteraceae, Acetobacteraceae, Beijerinckiaceae, and Koribacteraceae were present in greater proportions than in CR rhizosphere soils from the –Al site (Fig. 1B and Supplementary Table S2). No significant differences were detected in alpha-diversity metrics (Shannon Index, Pielou's evenness, Observed Features, and Faith's PD; $p > 0.05$) among samples (Supplementary Fig. S1).

Beta-diversity analysis (PERMANOVA) revealed that site was the main factor structuring bacterial communities (+ Al / –Al; $F = 5.55$, $R^2 = 0.24$, $p = 0.001$), whereas no significant differences were detected among soil sample types (CR, non-CR, and BS; $F = 1.52$, $R^2 = 0.13$, $p = 0.051$) or their interaction ($F = 1.39$, $R^2 = 0.12$, $p = 0.082$) (Fig. 1C; Supplementary Table S3). In the PCA ordination, samples from the + Al site clustered distinctly from those of the –Al site, with + Al samples showing visually tighter grouping compared to the broader dispersion observed among –Al samples. Functional predictions based on taxonomic annotation indicated that the dominant bacterial functional groups across all soil types and both sites were chemoheterotrophs and aerobic chemoheterotrophs. At the + Al site, a higher predicted representation of taxa associated with cellulolysis, phototrophy, and photoheterotrophy was observed, whereas at the –Al site, taxa linked to nitrate reduction, nitrogen respiration, and nitrate respiration were more frequently predicted (Fig. 1D).

According to the ZIGMM analysis, *Candidatus Udaeobacter* was significantly more abundant at the − Al site across all sample types, with relative abundances of 8.2% in CR, 9.8% in non-CR, and 10.7% in BS, compared to ≤ 1.6% in the corresponding + Al samples (Fig. 2A–C). Conversely, *Candidatus Xiphinematobacter* was significantly enriched in CR (5.8%) and non-CR (6.0%) rhizosphere samples at the + Al site relative to the − Al site (2.2% and 2.9%, respectively), while it was not differentially abundant in BS (Fig. 2A, B and C).

Isolation and relative abundance of Al-tolerant bacteria

At the -Al site, Al-tolerant bacterial strains were found exclusively in the rhizosphere soil CR of *G. avellana* (Fig. 3A). In contrast, at the + Al site, these strains occurred in both bulk soil and the CR rhizosphere, with greater abundance in the latter; however, no Al-tolerant isolates were detected in the non-CR rhizosphere. (Fig. 3B). Furthermore, bacteria associated with CR of *G. avellana* growing at the -Al site showed greater abundance (1.5×10^6 CFU mL^{-1}) and a higher degree of tolerance to Al (300 mg L^{-1}, Fig. 3A) compared to those at the + Al site (8.2×10^5 CFU mL^{-1}), which showed tolerance up to 200 mg L^{-1} (Fig. 3B).

According to our selection criteria based on morphological characterization (Supplementary Table S4) and tolerance to ≥100 mg L^{-1} of Al, 11 strains were pre-selected. The genotyping by ERIC-PCR (Supplementary Fig. S2) and subsequent partial sequencing of 16S rRNA genes revealed the presence of bacteria belonging to the genera *Paeniglutamicibacter*, *Buttiauxella*, *Bacillus*, *Chryseobacterium*, *Pseudomonas*, *Arthrobacter*, *Serratia*, and *Rahnella* (Table 2).

Table 2. Identification of Al tolerant bacterial strains isolated from rhizosphere of cluster roots (CR) of *Gevuina avellana* and bulk soil (BS).

Site	Strain	16S rRNA		
		GenBank Accession	Closest known relative	% ID
Oncol Park				
(+ Al)	CR+Al01	PZ261622	*Paeniglutamicibacter antarticus*	98.59
	CR+Al03	PZ261623	*Buttiauxella* sp.	98.43
	CR+Al04	PZ261624	*Bacillus* sp.	100
	CR+Al02	PZ261625	*Buttiauxella* sp.	99.15
	BS+Al03	PZ261626	*Chryseobacterium* sp.	98.7
	BS+Al01	PZ261627	*Pseudomonas* sp.	99.15
	BS+Al05	PZ261628	*Arthrobacter* sp.	97.24
	BS+Al04	PZ261629	*Pseudomonas* sp.	99.35
Rucamanque Park				
(-Al)	CR-Al01	PZ261630	*Serratia proteamaculans*	99.88
	CR-Al04	PZ261631	*Serratia* sp.	100
	CR-Al05	PZ261632	*Rahnella victoriana*	98.7

3.4. *In vitro* screening of plant growth-promoting traits in bacterial isolates

A total of 11 bacterial strains were isolated from rhizospheric soil CR of *G. avellana* and from bulk soil, of which seven exhibited clear plant growth-promoting capabilities. Notably, *Buttiauxella* sp. (CR+Al02), *Buttiauxella* sp. (CR+Al03), *Pseudomonas* sp. (BS+Al01), *Pseudomonas* sp. (BS+Al04), *Serratia proteamaculans* (CR-Al01), *Serratia* sp. (CR-Al04) and *Rahnella victoriana* (CR-Al05) were identified as the most promising isolates. On the other hand, *Paeniglutamicibacter antarcticus* (CR+Al01), *Arthrobacter* sp. (BS+Al05), and *Bacillus* spp. (CR+Al04) strains were highlighted for producing only IAA and siderophores, respectively. Seven strains demonstrated the capacity to produce siderophores and to solubilize at least one of the P sources evaluated (Table 3). Of the 11 strains analyzed, 3 exhibited qualitative and quantitative ACC deaminase production and activity. The *Pseudomonas* sp. (BS+Al01) strain, isolated from BS at the + Al sampling site, stood out from the other bacterial isolates, showing 30% greater activity (Table 3). Among the 11 bacterial isolates evaluated, four showed detectable IAA production (Table 3). However, one of these strains exhibited concentrations below the detection limit of the method (< 0.2 mg L^{-1}). Of the four IAA-producing isolates, two were obtained from the + Al sampling site (Oncol): *Paeniglutamicibacter antarcticus* and *Arthrobacter* sp.; while the remaining two were collected from the –Al site (Rucamanque): *Serratia* sp. and *Serratia proteamaculans*. Regardless of sampling location, three of the four IAA-producing strains were isolated from the cluster roots (CR), specifically *Serratia* sp., *S. proteamaculans*, and *P. antarcticus*. Finally, it should be noted that the isolated *Chryseobacterium sp.* (BS+AL01) does not exhibit PGP traits; however, it is included in Table 3 as it is an Al-tolerant isolate.

Table 3
The Plant growth-promoting traits (PGPTs) of the Al-tolerant bacterial strains isolated from rhizosphere of cluster roots (CR) of Gevuina avellana and bulk soil.

Site	*Organism* (Isolate)	Siderophore	Phosphate solubilization				ACC deaminase[a]	IAA production[b]
			$FePO_4$	$Ca_3(PO_4)_2$	$AlPO_4$	Phosphate rock		
Oncol Park	*Paeniglutamicibacter antarticus* (CR+Al01)	-	-	-	-	-	-	0.47 ± 0.02
	Buttiauxella sp. (CR+Al02)	+	+	+	+	+	-	-
	Buttiauxella sp. (CR+Al03)	+	+	+	+	+	-	-
	Bacillus sp. (CR+Al04)	+	-	-	-	-	-	-
	Pseudomonas sp. (BS+Al01)	-	+	+	+	+	345.8 ± 64.9	-
	Chryseobacterium sp. (BS+Al03)	-	-	-	-	-	-	-
	Pseudomonas sp. (BS+Al04)	+	+	+	+	+	-	-
	Arthrobacter sp. (BS+Al05)	-	-	-	-	-	-	0.20 ± 0.01
Rucamanque Park	*Serratia proteamaculans* (CR-Al01)	+	-	-	+	-	191.5 ± 47.2	0.49 ± 0.03
	Serratia sp. (CR-Al04)	+	+	+	+	+	141.7 ± 14.1	0.52 ± 0.02
	Rahnella victoriana (CR-Al05)	+	+	+	+	+	-	-

[a] n mol α cb mg^{-1} protein h^{-1} 1-aminocyclopropane-1-carboxylate (ACC) deaminase activity

[b] mg L^{-1} indole-3-acetic acid (IAA) production

The ability to produce siderophores and to solubilize phosphate was represented by '+'and '–', where '+'means possesses activity and '–'means no activity.

Discussion

This study analyzed the bacterial community associated with *G. avellana* roots growing in native soils with contrasting Al saturation. Metabarcoding analysis revealed that the structure of the bacterial community was clearly separated between + Al and − Al sites. (Fig. 1C), indicating that site-specific soil conditions strongly influenced the soil microbiota, acting as a key environmental driver. This pattern is consistent with previous studies, which found that environmental factors (such as the presence of metals and the physicochemical conditions of the site) have a much greater impact on the structure of the microbial community than the plant species itself (Barra et al. 2019; Ma et al. 2022; Salam et al. 2020; Xing et al. 2024; Yang et al. 2012). In our study, the lower dispersion

among samples from the + Al site (Fig. 1C), indicate a more homogeneous bacterial community structure, likely due to a strong abiotic filtering imposed by high Al^{3+} availability and nutrient limitation (mainly by N, Table 1). In contrast, samples from the – Al site showed greater dispersion, suggesting higher variability in community compositions and a less restrictive edaphic environment that may support greater taxonomic heterogeneity and potential functional redundancy. This interpretation is consistent with previous findings high Al^{3+} concentrations, pH, and nutrient deficiencies, particularly depleted mineral nitrogen act as dominant environmental filters (He et al. 2012; Kang et al. 2024; Tripathi et al. 2018). These abiotic stresses likely drive deterministic assembly, reducing compositional variability and shifting the community structure, as evidenced by the loss of denitrifiers (bacteria involved in nitrate reduction, nitrogen respiration, and nitrate respiration) at the + Al site (see Fig. 1D).

At the phylum level, the most abundant bacterial groups across both sites were Proteobacteria, Acidobacteriota, and Planctomycetota, which together accounted for more than 60% of the total bacterial community (Supplementary Table S1). The relatively high abundance of Proteobacteria in rhizospheric samples (CR and non-CR) compared with BS suggests active recruitment of copiotrophic, metabolically versatile taxa, which are commonly associated with nutrient cycling, secondary metabolite production, and plant growth promotion in acidic or metal-rich environments (Kochian et al. 2015; Lian et al. 2019). Functional predictions using FAPROTAX further supported these patterns, revealing an enrichment of cellulolysis, phototrophy and photoheterotrophy functions in + Al rhizospheres (Fig. 1D), consistent with a microbiota adapted to both Al toxicity and probably also due to a greater availability of carbon derived from root exudates. However, it is important to note that FAPROTAX predictions are constrained by annotations derived from cultured organisms. Consequently, functional assignments for uncultured taxa are inferred from their closest taxonomic relatives and should be interpreted with caution, requiring further validation through complementary approaches such as metatranscriptomic analyses.

The secretion of carboxylates by roots of *G. avellana* (Delgado et al. 2021; Zúñiga-Feest et al. 2021) likely plays a central role in this selective recruitment by generating acidic microzones that favor Al-tolerant and metabolically active bacterial taxa. In contrast, the reduced relative abundance of Acidobacteriota in root-associated samples (Fig. 1A and Supplementary Table S1) compared with BS suggests an exclusion of oligotrophic taxa, which typically dominate nutrient-poor and low-energy environments. Planctomycetota maintained relatively stable abundance across sites and soil types (Fig. 1A and Supplementary Table S1), indicating a consistent contribution to essential processes, such as nitrogen and carbon turnover, under contrasting Al conditions. Additionally, the enrichment of taxa such as Ktedonobacteraceae in + Al sites (Fig. 1B and Supplementary Table S2) is consistent with previous studies showing increased relative abundance of these groups under conditions of high Al availability (Shi et al. 2020).

Regarding bacterial isolation, our results revealed the presence of several Al-tolerant bacteria genera harboring plant growth-promoting (PGP) traits. The isolates exhibiting PGP activities mainly belonged to the genera *Serratia*, *Paeniglutamicibacter, Rahnella*, *Buttiauxella*, *Bacillus*, *Arthrobacter*, and *Pseudomonas*, all of which are well recognized for their roles in enhancing plant growth under stressful soil conditions (Alexandre et al. 2021; Kusale et al. 2021; Liu et al. 2020; Wang et al. 2022; Yasmin et al. 2022). Previous studies have highlighted the role of *Bacillus* spp. and *Arthrobacter* spp. in promoting plant growth under high Al saturation conditions (Hazarika et al. 2023). Similarly, *Arthrobacter* spp. have been positively correlated with Al concentrations in acidic soils and have been shown to enhance plant growth in *Zingiber officinale* Roscoe, where Al toxicity is thought to select for microorganisms with enhanced plant growth-promoting capabilities (Zhang et al. 2020). In contrast, limited information is available regarding the role of *Paeniglutamicibacter* and *Buttiauxella* in promoting plant growth in soils with high Al availability.

It is widely known that plants interact with beneficial microorganisms inhabiting vital organs, establishing complex relationships with the native microbiota, from which the host selectively stimulates the growth and activity of specific taxa possessing beneficial traits (Philippot et al. 2013; Tharanath et al. 2024). The microorganisms isolated from the rhizosphere of CR of *G. avellana* possess functional traits that may contribute to plant growth and could be particularly relevant in soils with high Al availability, such as those found in the + Al site (Table 1). In addition, several bacterial strains isolated from the rhizosphere tolerated Al concentrations higher than 100 mg L^{-1}. Notably isolates obtained from CR-associated soil exhibited the highest tolerance levels, with some strains growing at concentrations up to 300 mg L^{-1}, regardless of the Al concentration measured in the original soil samples (Fig. 3). These tolerance values are in line with those described by Jiang et al. (2022), who point out that *Camelia sinensis*, an Al-hyperaccumulator plant, has endophytic bacteria in its roots and rhizospheric soil with an Al-tolerance reaching 200 mg L^{-1}. A concentration of available Al above 270 mg L^{-1} is considered highly toxic for most bacteria (Huang et al. 2018). Therefore, it is deduced that the CR of *G. avellana* are attracting or selecting Al-tolerant bacteria in their rhizosphere. Greater abundance of Al-tolerant bacteria at the -Al site could be attributed to less restrictive soil conditions, enabling the persistence of strains with more robust tolerance. Another possibility is that CR-exuded carboxylate concentrations vary between sites. Both hypotheses require further study.

According to our results, most bacterial isolates exhibited one or more PGP traits, including IAA production, phosphate solubilization, and siderophore secretion (Table 3). These functions are critical for plant adaptation to acidic soils, as siderophores can chelate toxic Al^{3+} ions, enhancing phosphate solubilization, and IAA stimulates root development under stress conditions (Lemire et al. 2010; Martínez et al. 2011). The prevalence of multifunctional PGP strains in + Al site suggests a co-adaptive relationship between *G. avellana* and its rhizosphere microbiota, in which bacterial mutualists play a key role in mitigating Al toxicity and sustaining plant fitness in highly acidic environments. One key mechanism explaining the selective recruitment of functional microorganisms is the continuous exudation of carboxylates by cluster roots. As reported by Renderos et al. (2022), microbial communities inhabiting the rhizosphere soil of CR of *E. coccineum* differ markedly from those in non-rhizospheric soils, largely due to the quantity and composition of root exudates released into the surrounding soil environment. The large amount of organic acids exuded by plants forming CR not only enhances soil nutrient availability but also provides a readily available carbon source for rhizospheric microorganisms (Sasse et al. 2018), thereby stimulating the proliferation of specific bacterial taxa with crucial roles in plant development.

One important mechanism of Al tolerance in bacteria is siderophore production, which was detected in seven of the analyzed isolates. In fact, previous studies have shown a strong correlation between Al tolerance and siderophore synthesis (Shilpi Mittal et al. 2003). Siderophores are low-molecular-weight compounds (500–1500 Da) with high affinity and selectivity for ferric iron (Fe^{3+}), facilitating iron uptake under Fe-limited conditions (Carrano et al. 1996; Timofeeva et al. 2022). Given the similar ionic radii of Al^{3+} and Fe^{3+} (54 and 64 pm, respectively) (Yokel 2002), some siderophores are also capable of binding Al and other metals, including copper, zinc, chromium, lead, manganese, cadmium, vanadium, gallium, and indium (Baysse et al. 2000; Cornelis 2008). Accordingly, siderophore-producing bacteria may possess effective Al detoxification mechanisms via Al^{3+} chelation (Mora et al. 2017). Aluminum tolerance in several isolates is likely associated with their siderophore-producing capacity, supporting their potential role in promoting plant growth under Al stress (Farh et al. 2017).

Phosphate solubilization by rhizospheric bacteria represents another key mechanism contributing to plant growth in acidic soils, where P availability is often severely limited (Rodríguez and Fraga 1999). Phosphate-solubilizing bacteria (PSB) release organic acids that acidify the rhizosphere and convert insoluble phosphate compounds into plant-available forms (Rodríguez and Fraga 1999). This process not only improves P nutrition but can also enhance plant tolerance to Al toxicity, as organic acids are able to chelate Al^{3+} and reduce its phytotoxic effects (He et al. 2019). Thus, the interaction between PSB and rhizosphere associated with CR of *G. avellana* may play a fundamental role in plant adaptation and survival in acidic soils with high Al availability, improving both mineral nutrition and tolerance to abiotic stress. In this context, the isolate *Rahnella victoriana* (CR-Al 05) was particularly notable, producing phosphate-solubilization halos up to three times larger than those of other strains across the four phosphate sources tested (Supplementary Table S5). Recent studies have highlighted the plant growth-promoting potential of *Rahnella* spp. (Alvarado et al. 2024). For instance, *R. victoriana* strain B38 promotes growth in *Brassica napus* and enhances *Arabidopsis* performance under arsenic stress (Yan et al. 2024). Similarly, *R. victoriana* strain JZ-GX1 has been shown to promote growth in *Pinus massoniana* through siderophore production, IAA synthesis, nitrogen fixation, and P and potassium solubilization (Kong et al. 2022). Notably, *P. massoniana*, like *G. avellana*, grows in acidic soils, underscoring the ecological relevance of this bacterial species and supporting the need for further studies on its interactions with *G. avellana*.

Additional PGPTs were also detected, including ACC deaminase activity and IAA production. In this study, four out of eleven isolates produced IAA under the tested culture conditions, most of which belonged to the genus *Serratia*. Numerous studies have demonstrated the potential of *Serratia* spp. as PGPT. (Dastager et al. 2011; George et al. 2013), and strains belonging to this genus have previously been isolated from the rhizosphere of plants growing in Chilean volcanic soils (Jorquera et al. 2014; Martínez et al. 2011). Together, these findings indicate that *Serratia* spp. and other multifunctional bacteria identified in this study possess significant potential to enhance plant growth in acidic, Al-rich soils.

Taken together, these findings demonstrate that *G. avellana* maintains a structured and functionally resilient microbiota even under high Al saturation, highlighting a close ecological association between the host plant and its rhizosphere bacterial communities. Our results suggest that the presence of Al-tolerant and metabolically versatile bacteria may contribute to plant persistence and performance in acidic soils. From an applied perspective, the isolation of Al-tolerant bacteria exhibiting PGPT opens new opportunities for developing bioinoculants to improve crop productivity and soil health in acidic or Al-rich environments. Moreover, *G. avellana* emerges as a valuable model species for investigating plant-microbe interactions in acidic soils, with broader implications for ecological restoration and the development of sustainable biotechnological strategies for metal-stressed ecosystems.

Conclusions

This study provides the first characterization of the bacterial community associated with cluster roots (CR) of the Al-hyperaccumulator *Gevuina avellana* growing under contrasting soil Al saturation in southern Chile. Our findings reveal that soil chemical properties, particularly Al saturation, pH, and nutrient availability, were the primary drivers of bacterial community structure, overriding any effect of root type or soil compartment (CR, non-CR and BS). High Al availability acted as a strong environmental filter, selecting for a more homogeneous bacterial assemblage dominated by Al-adapted taxa such as Ktedonobacteraceae and *Candidatus Xiphinematobacter*. Beyond community-level patterns, the rhizosphere of CR emerged as a selective niche for Al-tolerant bacteria, harboring isolates with tolerance levels reaching up to 300 mg L^{-1} regardless of the Al concentration in the native soil. Notably, isolates from the low-Al site exhibited higher tolerance than those from the + Al site, pointing to a complex interplay between soil chemistry, root exudation, and microbial selection that warrants further investigation. Most of these isolates also displayed multiple plant growth-promoting traits, including siderophore production, phosphate solubilization, ACC deaminase activity, and IAA synthesis with *Serratia spp*. and *Rahnella victoriana* standing out as multifunctional candidates with potential biotechnological applications. Taken together, these results highlight *G. avellana* as a valuable model for studying plant–microbe interactions in acidic, Al-rich soils and open new avenues for developing bioinoculants aimed at improving crop productivity in Al-stressed Andisols. Future work should validate the plant growth-promoting potential of these isolates under controlled and field conditions and explore the mechanistic links between CR exudation patterns and microbial recruitment.

Declarations

Acknowledgments

The authors acknowledge Rucamanque Ecological and Cultural Park and Oncol Park to collect soil samples.

M. Delgado thanks to FONDECYT Regular Project N° 1210684. M. Reyes-Díaz thanks to ANID/ANILLO/ATE250064. H. Herrera thanks to ANID FONDEF ID25I10565, ANID FONDECYT Regular 1261677, and ANID Desafíos Recuperación Post-Incendios PINC230004. Furthermore, the authors acknowledge the supercomputing infrastructure of Soroban (SATREPS MACH-JPM/JSA1705) at “Centro de Modelación y Computación Científica at Universidad de La Frontera”.

Funding

This study was funded by the “Agencia Nacional de Investigación y Desarrollo” (ANID), FONDECYT Initiation Project N° 11220462

Competing interesting

The authors declare that they have no conflict of interest.

Authors contributions

Graciela Berríos and Mabel Delgado contributed to the study conception and design. Material preparations, data collection and analysis were performed by Graciela Berríos, Jaznine Sandoval, Vicente Arellano, Carla Sandoval, Claudia Rabert and Marcia Astorga-Eló. The bioinformatics analysis, data processing and statistical validation was performed by Giovanni Larama. The first draft of the manuscript was written by Graciela Berríos, Claudia Rabert and Héctor Herrera. Mabel Delgado and Marjorie Reyes Díaz revised and corrected it. All authors read and approved of the final manuscript.

Data Availability

The datasets generated during the current study are available in the NCBI repository. Raw 16S rRNA gene amplicon sequences have been deposited in the NCBI Sequence Read Archive (SRA) under BioProject accession number PRJNA1449941 (https://www.ncbi.nlm.nih.gov/bioproject/PRJNA1449941). All other data supporting the findings of this study are included in this article and its supplementary materials.

References

1. Ahemad M (2019) Remediation of metalliferous soils through the heavy metal resistant plant growth promoting bacteria: paradigms and prospects. Arab J Chem 12:1365–1377

2. Alexandre FS, Della Flora LV, Henrique IG, da Silva DC, Mercedes AP, Cardoso Silva A, Silva de Oliveira A, Bondespacho da Silva MP, Formelh Ronning BP, Dreher DR (2021) Arbuscular mycorrhizal fungi (Rhizophagus clarus) and rhizobacteria (Bacillus subtilis) can improve the clonal propagation and development of teak for commercial plantings. Front Plant Sci 12:628769
3. Alvarado R, Sagredo-Saez C, Fuentes-Quiroz A, Villanueva-Guerrero A, Mujica MI, Ahumada R, Almonacid-Muñoz L, Jorquera-Fontena E, de Oliveira Costa PH, da Silva Valadares RB (2024) Endophytic seed-associated microbial diversity and its impact on seedling growth of the Andean tree Nothofagus obliqua (Mirb.) Oerst. Plant Growth Regul : 1–16
4. Anderson MJ (2001) A new method for non-parametric multivariate analysis of variance. Austral Ecol 26:32–46
5. Barone P, Rosellini D, LaFayette P, Bouton J, Veronesi F, Parrott W (2008) Bacterial citrate synthase expression and soil aluminum tolerance in transgenic alfalfa. Plant Cell Rep 27:893–901
6. Barra PJ, Pontigo S, Delgado M, Parra–Almuna L, Duran P, Valentine AJ, Jorquera MA, de la Luz Mora M (2019) Phosphobacteria inoculation enhances the benefit of P–fertilization on *Lolium perenne* in soils contrasting in P–availability. Soil Biol Biochem 136:107516. 10.1016/j.soilbio.2019.06.012
7. Bashan Y, Holguin G, De-Bashan LE (2004) Azospirillum-plant relationships: physiological, molecular, agricultural, and environmental advances (1997–2003). Can J Microbiol 50:521–577
8. Baysse C, De Vos D, Naudet Y, Vandermonde A, Ochsner U, Meyer J-M, Budzikiewicz H, Schäfer M, Fuchs R, Cornelis P (2000) Vanadium interferes with siderophore-mediated iron uptake in Pseudomonas aeruginosa. Microbiology 146:2425–2434
9. Bojórquez-Quintal E, Escalante-Magaña C, Echevarría-Machado I, Martínez-Estévez M (2017) Aluminum, a friend or foe of higher plants in acid soils. Front Plant Sci 8:1767
10. Bolyen E, Rideout JR, Dillon MR, Bokulich NA, Abnet CC, Al-Ghalith GA, Alexander H, Alm EJ, Arumugam M, Asnicar F (2019) Reproducible, interactive, scalable and extensible microbiome data science using QIIME 2. Nat Biotechnol 37:852–857
11. Bürgmann H, Meier S, Bunge M, Widmer F, Zeyer J (2005) Effects of model root exudates on structure and activity of a soil diazotroph community. Environ Microbiol 7:1711–1724
12. Callahan BJ, McMurdie PJ, Rosen MJ, Han AW, Johnson AJA, Holmes SP (2016) DADA2: High-resolution sample inference from Illumina amplicon data. Nat Methods 13:581–583. 10.1038/nMeth.3869
13. Carrano CJ, Drechsel H, Kaiser D, Jung G, Matzanke B, Winkelmann G, Rochel N, Albrecht-Gary AM (1996) Coordination chemistry of the carboxylate type siderophore rhizoferrin: the iron (III) complex and its metal analogs. Inorg Chem 35:6429–6436
14. Cornelis P (2008) Unexpected interaction of a siderophore with aluminum and its receptor. J Bacteriol 190:6541–6543
15. Cristancho R, Hanafi M, Syed Omar S, Rafii M (2011) Variations in oil palm (Elaeis guineensis Jacq.) progeny response to high aluminium concentrations in solution culture. Plant Biol 13:333–342
16. Chaparro JM, Badri DV, Bakker MG, Sugiyama A, Manter DK, Vivanco JM (2013) Root exudation of phytochemicals in Arabidopsis follows specific patterns that are developmentally programmed and correlate with soil microbial functions. PLoS ONE 8:e55731
17. Chenery EM (1948) Aluminium in the plant world. Part I, General survey in dicotyledons. Kew Bull 3:173–183
18. Dastager SG, Deepa C, Pandey A (2011) Potential plant growth-promoting activity of Serratia nematodiphila NII-0928 on black pepper (Piper nigrum L). World J Microbiol Biotechnol 27:259–265
19. Delgado M, Barra P, Habermann G, Valdebenito D, Ryan PR, Reyes-Díaz M, Mora M (2025) Prospecting the presence of aluminum-accumulating species inhabiting temperate rainforests from southern Chile. Plant Soil 515:393–406. 10.1007/s11104-025-07592-3
20. Delgado M, Barra PJ, Berrios G, Mora ML, Duran P, Valentine A, Reyes-Díaz M (2024) Do aluminum (Al)-hyperaccumulator and phosphorus (P)-solubilising species assist neighbouring plants sensitive to Al toxicity and P deficiency? Front Plant Sci 15:1371123. 10.3389/fpls.2024.1371123
21. Delgado M, Valle S, Barra PJ, Reyes-Díaz M, Zúñiga-Feest A (2019) New aluminum hyperaccumulator species of the Proteaceae family from southern South America. Plant Soil 444:475–487
22. Delgado M, Valle S, Reyes-Díaz M, Barra PJ, Zúñiga-Feest A (2018) Nutrient use efficiency of southern South America Proteaceae species. Are there general patterns in the Proteaceae family? Front Plant Sci 9:883
23. Delgado M, Zúñiga-Feest A, Reyes-Díaz M, Barra P, Ruiz S, Bertin-Benavides A, Valle S, Pereira M, Lambers H (2021) Ecophysiological performance of Proteaceae species from southern South America growing on substrates derived from young volcanic materials. Front Plant Sci 12:636056

24. Durán P, Acuña JJ, Jorquera MA, Azcón R, Paredes C, Rengel Z, de la Luz Mora M (2014) Endophytic bacteria from selenium-supplemented wheat plants could be useful for plant-growth promotion, biofortification and Gaeumannomyces graminis biocontrol in wheat production. Biol Fertil Soils 50:983–990
25. Dworkin M, Foster J (1958) Experiments with some microorganisms which utilize ethane and hydrogen. J Bacteriol 75:592–603
26. Farh ME-A, Kim Y-J, Sukweenadhi J, Singh P, Yang D-C (2017) Aluminium resistant, plant growth promoting bacteria induce overexpression of Aluminium stress related genes in Arabidopsis thaliana and increase the ginseng tolerance against Aluminium stress. Microbiol Res 200:45–52
27. George P, Gupta A, Gopal M, Thomas L, Thomas GV (2013) Multifarious beneficial traits and plant growth promoting potential of Serratia marcescens KiSII and Enterobacter sp. RNF 267 isolated from the rhizosphere of coconut palms (Cocos nucifera L). World J Microbiol Biotechnol 29:109–117
28. Hazarika DJ, Bora SS, Naorem RS, Sharma D, Boro RC, Barooah M (2023) Genomic insights into Bacillus subtilis MBB3B9 mediated aluminium stress mitigation for enhanced rice growth. Sci Rep 13:16467
29. He G, Wu J, Liu Q, Zhang J (2012) Microbial and enzyme properties of acidic red soils under aluminum stress. Fresenius Environ Bull 21:2818–2825
30. He H, Li Y, He L-F (2019) Role of nitric oxide and hydrogen sulfide in plant aluminum tolerance. Biometals 32:1–9
31. Hu Q-P, Xu J-G (2011) A simple double-layered chrome azurol S agar (SD-CASA) plate assay to optimize the production of siderophores by a potential biocontrol agent Bacillus. Afr J Microbiol Res 5:4321–4327
32. Huang S, Xiaodong W, Xu L, Genhe H, Jichun W (2018) Isolation, identification, and characterization of an aluminum-tolerant bacterium Burkholderia sp. SB1 from an acidic red soil. Pedosphere 28:905–912
33. Jansen S, Broadley MR, Robbrecht E, Smets E (2002) Aluminum hyperaccumulation in Angiosperms: A review of its phylogenetic significance. Bot Rev 68:235–269. 10.1663/0006-8101
34. Jiang X, Li W-W, Han M, Chen G, Wu J, Lai S, Fu Z, Zhang S, Deng W-W, Gao L (2022) Aluminum-tolerant, growth-promoting endophytic bacteria as contributors in promoting tea plant growth and alleviating aluminum stress. Tree Physiol 42:1043–1058
35. Jorquera MA, Inostroza NG, Lagos LM, Barra PJ, Marileo LG, Rilling JI, Campos DC, Crowley DE, Richardson AE, Mora ML (2014) Bacterial community structure and detection of putative plant growth-promoting rhizobacteria associated with plants grown in Chilean agro-ecosystems and undisturbed ecosystems. Biol Fertil Soils 50:1141–1153
36. Kang H, Xue Y, Cui Y, Moorhead DL, Lambers H, Wang D (2024) Nutrient limitation mediates soil microbial community structure and stability in forest restoration. Sci Total Environ 935:173266
37. Katoh K, Standley DM (2013) MAFFT multiple sequence alignment software version 7: improvements in performance and usability. Mol Biol Evol 30:772–780
38. Kavamura VN, Esposito E (2010) Biotechnological strategies applied to the decontamination of soils polluted with heavy metals. Biotechnol Adv 28:61–69
39. Kochian LV, Hoekenga OA, Pineros MA (2004) How do crop plants tolerate acid soils? Mechanisms of aluminum tolerance and phosphorous efficiency. Annu Rev Plant Biol 55:459–493
40. Kochian LV, Piñeros MA, Liu J, Magalhaes JV (2015) Plant adaptation to acid soils: the molecular basis for crop aluminum resistance. Annu Rev Plant Biol 66:571–598. 10.1146/annurev-arplant-043014-114822
41. Kong W-L, Wang W-Y, Zuo S-H, Wu X-Q (2022) Genome sequencing of Rahnella victoriana JZ-GX1 provides new insights into molecular and genetic mechanisms of plant growth promotion. Front Microbiol 13:828990
42. Kusale SP, Attar YC, Sayyed R, Malek RA, Ilyas N, Suriani NL, Khan N, El Enshasy HA (2021) Production of plant beneficial and antioxidants metabolites by Klebsiella variicola under salinity stress. Molecules 26:1894
43. Lambers H, Shane MW, Cramer MD, Pearse SJ, Veneklaas EJ (2006) Root structure and functioning for efficient acquisition of phosphorus: Matching morphological and physiological traits. Ann Bot 98:693–713. 10.1093/aob/mcl114
44. Lemire J, Mailloux R, Auger C, Whalen D, Appanna VD (2010) Pseudomonas fluorescens orchestrates a fine metabolic-balancing act to counter aluminium toxicity. Environ Microbiol 12:1384–1390
45. Lian T, Ma Q, Shi Q, Cai Z, Zhang Y, Cheng Y, Nian H (2019) High aluminum stress drives different rhizosphere soil enzyme activities and bacterial community structure between aluminum-tolerant and aluminum-sensitive soybean genotypes. Plant Soil 440:409–425

46. Liu A, Zhang P, Bai B, Bai F, Jin T, Ren J (2020) Volatile organic compounds of endophytic Burkholderia pyrrocinia strain JK-SH007 promote disease resistance in poplar. Plant Dis 104:1610–1620
47. López D, Barra P, Valdebenito D, Duran P, Yan L, Lambers H, Mora M, Delgado M (2025) Leaf manganese concentrations as a proxy for root carboxylate exudation: a first survey in phosphorus-limited South American temperate rainforests. Plant Soil 1–21. 10.1007/s11104-025-07825-5
48. Louca S, Parfrey LW, Doebeli M (2016) Decoupling function and taxonomy in the global ocean microbiome. Science 353: 1272–1277. doi: 0.1126/science.aaf450
49. Louden BC, Haarmann D, Lynne AM (2011) Use of blue agar CAS assay for siderophore detection. J Microbiol biology Educ 12:51–53
50. Ma W, Tang S, Dengzeng Z, Zhang D, Zhang T, Ma X (2022) Root exudates contribute to belowground ecosystem hotspots: A review. Front Microbiol 13:937940
51. Ma Y (2017) Beneficial bacteria for disease suppression and plant growth promotion. Plant-Microbe Interactions in Agro-Ecological Perspectives: Volume 1: Fundamental Mechanisms, Methods and Functions: 513–529
52. Marschner P, Crowley D, Yang CH (2004) Development of specific rhizosphere bacterial communities in relation to plant species, nutrition and soil type. Plant Soil 261:199–208. 10.1023/B:PLSO.0000035569.80747.c5
53. Marschner P, Grierson PF, Rengel Z (2005) Microbial community composition and functioning in the rhizosphere of three Banksia species in native woodland in Western Australia. Appl Soil Ecol 28:191–201. 10.1016/j.apsoil.2004.09.001
54. Martínez OA, Jorquera MA, Crowley DE, de la Luz Mora M (2011) Influence of nitrogen fertilisation on pasture culturable rhizobacteria occurrence and the role of environmental factors on their potential PGPR activities. Biol Fertil Soils 47:875–885
55. Medel F, Donoso C, Halloy S, Donoso C, Premoli A, Gallo L, Ipinza R (2004) Variación en Gevuina avellana Mol. Variabilidad intraespecífica de las especies de los bosques templados de Chile y Argentina. Editorial Universitaria, Santiago de Chile, pp 326–352
56. Medel F, Medel R (2000) Gevuina avellana Mol: características y mejoramiento genético de un frutal de nuez nativo para el mercado internacional
57. Meliani A, Bensoltane A, Benidire L, Oufdou K (2017) Plant growth-promotion and IAA secretion with Pseudomonas fluorescens and Pseudomonas putida. Research & Reviews: Journal of Botanical Sciences 6: 16–24
58. Mora ML, Demanet R, Acuña JJ, Viscardi S, Jorquera M, Rengel Z, Durán P (2017) Aluminum-tolerant bacteria improve the plant growth and phosphorus content in ryegrass grown in a volcanic soil amended with cattle dung manure. Appl Soil Ecol 115:19–26
59. Morgan J, Bending G, White P (2005) Biological costs and benefits to plant–microbe interactions in the rhizosphere. J Exp Bot 56:1729–1739
60. Nautiyal CS (1999) An efficient microbiological growth medium for screening phosphate solubilizing microorganisms. FEMS Microbiol Lett 170:265–270
61. Oksanen J, Blanchet FG, Friendly M, Kindt R, Legendre P, McGlinn D, Minchin PR, O'hara R, Simpson GL, Solymos P (2019) vegan: Community Ecology Package. R package version 2.5-6
62. Oleńska E, Małek W, Wójcik M, Swiecicka I, Thijs S, Vangronsveld J (2020) Beneficial features of plant growth-promoting rhizobacteria for improving plant growth and health in challenging conditions: A methodical review. Sci Total Environ 743:140682
63. Osawa H, Ikeda S, Tange T (2013) The rapid accumulation of aluminum is ubiquitous in both the evergreen and deciduous leaves of Theaceae and Ternstroemiaceae plants over a wide pH range in acidic soils. Plant Soil 363:49–59. 10.1007/s11104-012-1285-5
64. Paulson JN, Stine OC, Bravo HC, Pop M (2013) Differential abundance analysis for microbial marker-gene surveys. Nat Methods 10:1200–1202. 10.1038/nmeth.2658
65. Peace TA, Brock KV, Stills HF Jr (1994) Comparative analysis of the 16S rRNA gene sequence of the putative agent of proliferative ileitis of hamsters. Int J Syst Evol MicroBiol 44:832–835
66. Penrose DM, Glick BR (2003) Methods for isolating and characterizing ACC deaminase-containing plant growth-promoting rhizobacteria. Physiol Plant 118:10–15
67. Philippot L, Raaijmakers JM, Lemanceau P, van der Putten WH (2013) Going back to the roots: the microbial ecology of the rhizosphere. Nat Rev Microbiol 11:789–799. 10.1038/nrmicro3109
68. Price MN, Dehal PS, Arkin AP (2010) FastTree 2–approximately maximum-likelihood trees for large alignments. PLoS ONE 5:e9490

69. Quast C, Pruesse E, Yilmaz P, Gerken J, Schweer T, Yarza P, Peplies J, Glöckner FO (2012) The SILVA ribosomal RNA gene database project: improved data processing and web-based tools. Nucleic Acids Res 41:D590–D596. 10.1093/nar/gks1219
70. Rafiee M, Bara M, Stephens C, Blackall P (2000) Application of ERIC PCR for the comparison of isolates of Haemophilus parasuis. Aust Vet J 78:846–849
71. Renderos L, Zúñiga-Feest A, Delgado M, Muñoz G, Carú M, Orlando J (2022) Cluster roots of Embothrium coccineum growing under field conditions differentially shape microbial diversity according to their developmental stage. J Soil Sci Plant Nutr 22:2418–2433
72. Rodríguez H, Fraga R (1999) Phosphate solubilizing bacteria and their role in plant growth promotion. Biotechnol Adv 17:319–339
73. Sadzawka R, Grez Z, Mora G, Saavedra R, Carrasco R, Rojas W (2004) Métodos de análisis recomendados para los suelos chilenos
74. Salam LB, Obayori OS, Ilori MO, Amund OO (2020) Effects of cadmium perturbation on the microbial community structure and heavy metal resistome of a tropical agricultural soil. Bioresources Bioprocess 7:25
75. Sanhueza T, Hernández I, Sagredo-Sáez C, Villanueva-Guerrero A, Alvarado R, Mujica MI, Fuentes-Quiroz A, Menendez E, Jorquera-Fontena E, Valadares RBS (2024) Juvenile plant–microbe interactions modulate the adaptation and response of forest seedlings to rapid climate change. Plants 13:175
76. Sarker PK, Karmoker D, Saha AK (2022) Bacterial associations with rice plants: Their diversity, abundance and importance in rice life cycle. Afr J Biol Sci 4:1–18
77. Sasse J, Martinoia E, Northen T (2018) Feed your friends: do plant exudates shape the root microbiome? Trends Plant Sci 23:25–41
78. Segata N, Izard J, Waldron L, Gevers D, Miropolsky L, Garrett WS, Huttenhower C (2011) Metagenomic biomarker discovery and explanation. Genome Biol 12:1–18
79. Shi Q, Jin J, Liu Y, Zhang Y, Cai Z, Ma Q, Cheng Y, Wen R, Nian H, Lian T (2020) High aluminum drives different rhizobacterial communities between aluminum-tolerant and aluminum-sensitive wild soybean. Frontiers in microbiology 11: 1996
80. Shilpi Mittal SM, Meyer J-M, Reeta Goel RG (2003) Isolation and characterization of aluminium and copper resistant'P'solubilizing alkalophilic bacteria
81. Silva I, Novais R, Jham G, Barros N, Gebrim F, Nunes F, Neves J, Leite F (2004) Responses of eucalypt species to aluminum: the possible involvement of low molecular weight organic acids in the Al tolerance mechanism. Tree Physiol 24:1267–1277
82. Sukweenadhi J, Kim Y-J, Choi E-S, Koh S-C, Lee S-W, Kim Y-J, Yang DC (2015) Paenibacillus yonginensis DCY84T induces changes in Arabidopsis thaliana gene expression against aluminum, drought, and salt stress. Microbiol Res 172:7–15
83. Tharanath AC, Upendra RS, Rajendra K (2024) Soil Symphony: A Comprehensive Overview of Plant–Microbe Interactions in Agricultural Systems. Appl Microbiol Biotechnol 4:1549–1567. 10.3390/applmicrobiol4040106
84. Timofeeva AM, Galyamova MR, Sedykh SE (2022) Bacterial siderophores: classification, biosynthesis, perspectives of use in agriculture. Plants 11:3065
85. Tripathi BM, Stegen JC, Kim M, Dong K, Adams JM, Lee YK (2018) Soil pH mediates the balance between stochastic and deterministic assembly of bacteria. ISME J 12:1072–1083
86. Wang C, Zhao X-Q, Shen R-F (2013) High aluminum tolerance of Rhodotorula sp. RS1 is associated with thickening of the cell wall rather than chelation of aluminum ions. Pedosphere 23:29–38
87. Wang Y-H, Hou L-L, Wu X-Q, Zhu M-L, Dai Y, Zhao Y-J (2022) Mycorrhiza helper bacterium Bacillus pumilus HR10 improves growth and nutritional status of Pinus thunbergii by promoting mycorrhizal proliferation. Tree Physiol 42:907–918
88. Xing W, Gai X, Xue L, Li S, Zhang X, Ju F, Chen G (2024) Enriched rhizospheric functional microbiome may enhance adaptability of Artemisia lavandulaefolia and Betula luminifera in antimony mining areas. Front Microbiol 15:1348054
89. Yan Y, Chang W, Tian P, Chen J, Jiang J, Dai X, Jiang T, Luo F, Yang C (2024) Exploring native arsenic (As)-resistant bacteria: unveiling multifaceted mechanisms for plant growth promotion under As stress. J Appl Microbiol 135:lxae228
90. Yang T, Ding Y, Zhu Y, Li Y, Wang X, Yang R, Lu G, Qi J, Yang Y (2012) Rhizosphere bacteria induced by aluminum-tolerant and aluminum-sensitive soybeans in acid soil
91. Yasmin H, Bano A, Wilson NL, Nosheen A, Naz R, Hassan MN, Ilyas N, Saleem MH, Noureldeen A, Ahmad P (2022) Drought-tolerant Pseudomonas sp. showed differential expression of stress-responsive genes and induced drought tolerance in Arabidopsis thaliana. Physiol Plant 174:e13497
92. Yokel RA (2002) Aluminum chelation principles and recent advances. Coord Chem Rev 228:97–113

93. Yu X, Li Y, Zhang C, Liu H, Liu J, Zheng W, Kang X, Leng X, Zhao K, Gu Y (2014) Culturable heavy metal-resistant and plant growth promoting bacteria in V-Ti magnetite mine tailing soil from Panzhihua, China. PLoS ONE 9:e106618
94. Zhang N, Ma Z, Li D, Ni H, Sun B, Liang Y (2022) Soil pH filters the association patterns of aluminum-tolerant microorganisms in rice paddies. Msystems 7:e01022–e01021. 10.1128/msystems.01022-21
95. Zhang S, Jiang Q, Liu X, Liu L, Ding W (2020) Plant growth promoting rhizobacteria alleviate aluminum toxicity and ginger bacterial wilt in acidic continuous cropping soil. Front Microbiol 11:569512
96. Zúñiga-Feest A, Sepúlveda F, Delgado M, Valle S, Muñoz G, Pereira M, Reyes-Diaz M (2021) Gevuina avellana and Lomatia dentata, two Proteaceae species from evergreen temperate forests of South America exhibit contrasting physiological responses under nutrient deprivation. Plant Soil 464:29–44

Figures

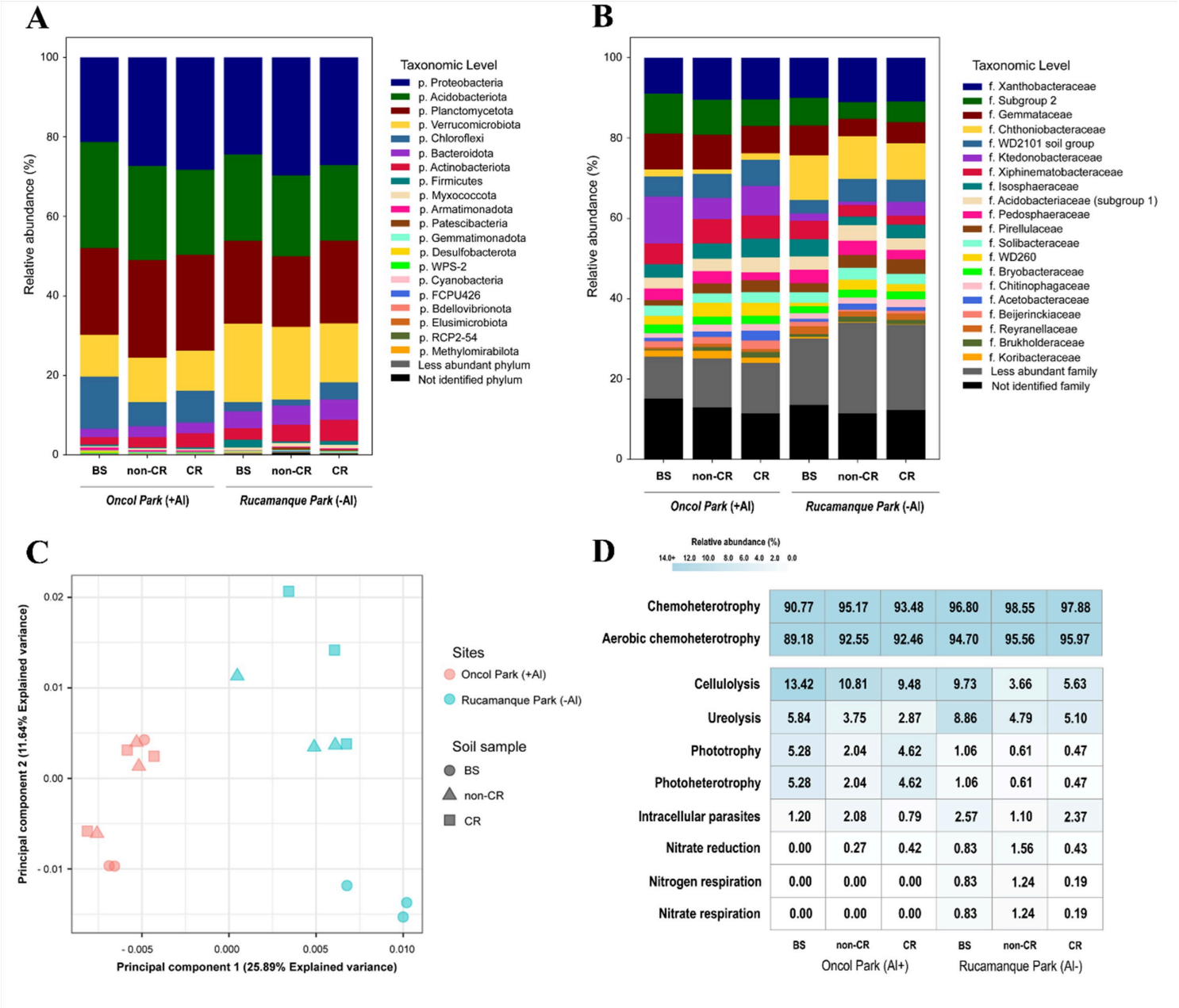


Figure 1

Taxonomic structure of bacterial communities associated with rhizospheric soil of *Gevuina avellana*(cluster roots, CR, and non-cluster roots, non-CR) and bulk soil (BS) collected at two sites with contrasting soil aluminium saturation (Rucamanque Park, –Al; Oncol Park,

+Al). Barplots show the relative abundance of the dominant bacterial phyla (A) and families (B). (C) Principal component analysis (PCA) illustrating differences among sites (Rucamanque Park, –Al; Oncol Park, +Al) and soil sample types (cluster roots: CR, non-cluster roots: non-CR, and Bulk soil: BS). (D) Predicted bacterial functional groups based on FAPROTAX. CR: rhizosphere soil of cluster roots of *G. avellana*; non-CR: rhizosphere soil of non-cluster roots of *G. avellana*; BS: bulk soil from native forest.

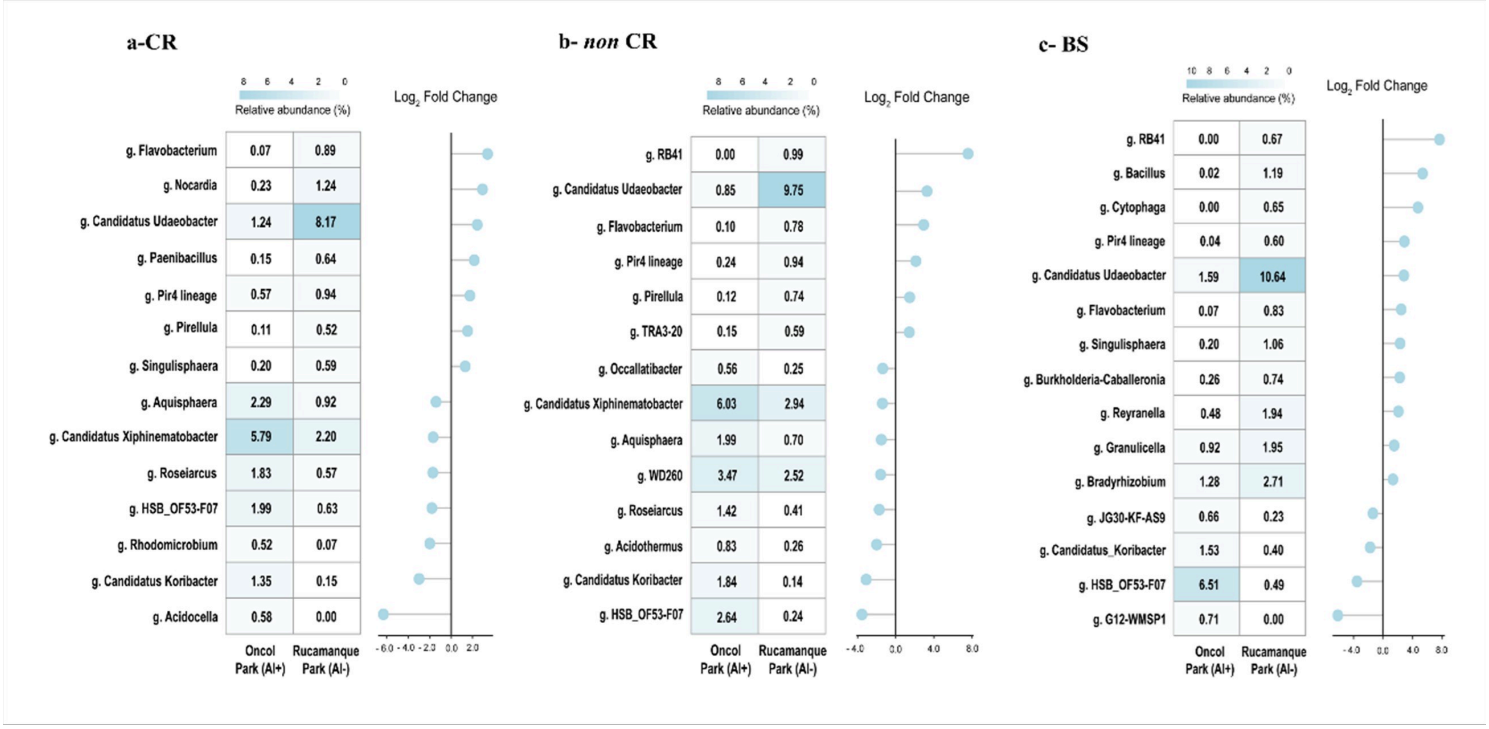


Figure 2

Heatmap of the relative abundance (%) from the most frequent bacterial genera (ZIGMM). Oncol Park (+Al) *vs.*Rucamanque Park (-Al). a-*CR*. Rhizosphere soil of cluster roots of *G. avellana. b-non-CR*. Rhizosphere soil of non-cluster roots of *G. avellana. c-BS*. Bacterial communities from the bulk soil (BS) of the native forest.

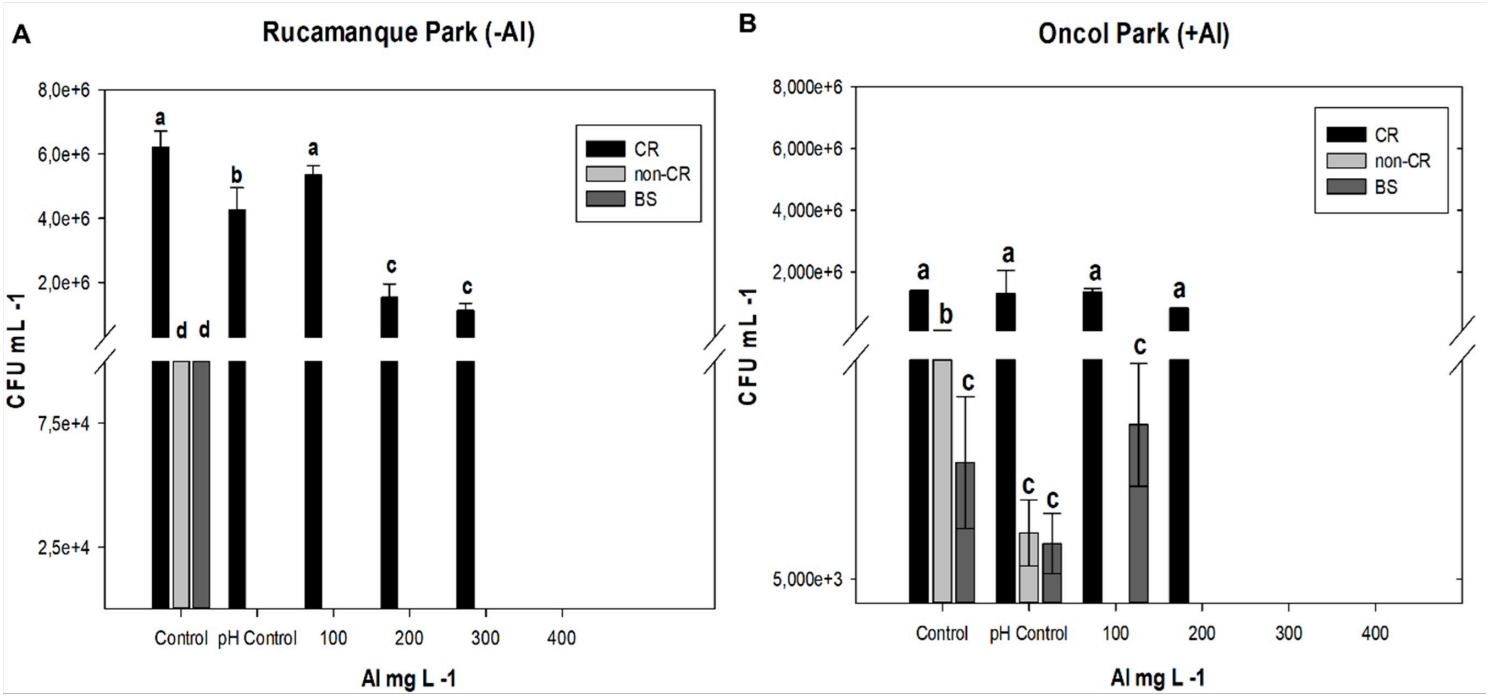


Figure 3

Bacterial abundance (CFU mL^{-1}) in rhizosphere of cluster roots (CR), non-cluster roots (non-CR), and bulk soil (BS) samples across different Al concentrations. Control: LB medium without Al. pH Control: LB medium without Al at pH 4.8. **A.** -Al Site, Rucamanque Park. **B**. +Al Site, Oncol Park. Different letters denote significant differences between treatments according to Tukey's test for mean comparison ($p \leq 0.05$).

Supplementary Files

This is a list of supplementary files associated with this preprint. Click to download.

- SupplementaryMaterial.docx